frontiers | Frontiers in Agronomy

TYPE Original Research
PUBLISHED 09 December 2025
DOI 10.3389/fagro.2025.1630354

OPEN ACCESS

EDITED BY
Mubasher Hussain,
Guangdong Pest control Technology Group, China

REVIEWED BY
Simone Pasinetti,
University of Brescia, Italy
Zain Mushtaq,
University of the Punjab, Pakistan

*CORRESPONDENCE
José Bruno Malaquias
malaquias.josebruno@gmail.com

RECEIVED 17 May 2025
ACCEPTED 24 October 2025
PUBLISHED 09 December 2025

CITATION
Silva AdS, de Oliveira R, Neto JSP, Borges VP, Guerrero MFC, Filho AACdA, Sousa RGC, Nascimento ARBd and Malaquias JB (2025) High-resolution suborbital remote sensing for detecting injuries caused by *Saccharicoccus sacchari* (Cockerell, 1895) (Hemiptera: Pseudococcidae) in sugarcane. *Front. Agron.* 7:1630354. doi: 10.3389/fagro.2025.1630354

High-resolution suborbital remote sensing for detecting injuries caused by *Saccharicoccus sacchari* (Cockerell, 1895) (Hemiptera: Pseudococcidae) in sugarcane

Allef de Souza Silva[1], Robério de Oliveira[1], Jacob Soares Pereira Neto[1], Valéria Peixoto Borges[1], Milton Fernando Cabezas Guerrero[2], André Augusto Castro do Amaral Filho[1], Rhadija Gracyelle Costa Sousa[1], Antônio Rogério Bezerra do Nascimento[3] and José Bruno Malaquias[1]*

[1]Entomology Laboratory, Federal University of Paraiba, Areia, PB, Brazil, [2]Entomology Laboratory, Universidade Técnica do Estado de Quevedo, Quevedo, Ecuador, [3]Department of Entomology and Acarology, ESALQ/USP, Piracicaba, São Paulo, Brazil

The pink mealybug (*Saccharicoccus sacchari*) is a significant pest of sugarcane, causing reductions in growth, sucrose content, and crop productivity. Its efficient management requires accurate field monitoring methods. This study evaluated the use of suborbital remote sensing with Remotely Piloted Aircraft (RPAs) in detecting injuries caused by this pest, using the vegetation indices NDVI and NDRE. The research was carried out in two periods (2023 and 2024), in an area of 1.5 hectares located in Alagoa Grande, Paraiba State, Brazil. Flights with a multispectral RPA and field surveys were conducted to determine the proportion of plants with low (<20 individuals/plant) and high infestation (>20 individuals/plant). Data were analyzed using both supervised and unsupervised machine learning methods. The results indicated a significant negative correlation between NDRE and low levels of infestation, while NDVI was more effective in detecting severe infestations. Multivariate analyses reinforced the complementarity of the indices in identifying the pest, with NDRE standing out in early detection and NDVI in identifying advanced damage. Kappa coefficients (> 0.80) comparing plant infestation with NRDE and NDVI yielded excellent results, with an overall Accuracy and Sensitivity of over 80.00% for the relationship between NDVI and high infestation per plant, and 73.33% and 83.33%, respectively, for NDRE with low infestation per plant. It is concluded that the integrated use of NDVI and NDRE, via remote sensing, is a promising tool for monitoring *S. sacchari* in sugarcane, contributing to faster and more efficient decision-making in pest management.

KEYWORDS

imaging, RPA, IPM, sampling, pink mealybug

1 Introduction

Sugarcane (interspecific *Saccharum hybrids*) is one of the most important crops in tropical and subtropical agroecosystems, with global socioeconomic prominence (Shang et al., 2024). Brazil leads the world in sugarcane production and exports, playing a crucial role in the national economy. In the 2023/24 harvest, the country harvested approximately 8.4 million hectares, resulting in a production of 713.2 million tons (Conab – Companhia Nacional de Abastecimento, 2024). However, crop productivity has been negatively impacted by the incidence of pests during the vegetative cycle, underscoring the need for effective monitoring to control them (Silva and Cavichioli, 2022).

Among the most relevant pests, the pink sugarcane mealybug (*Saccharicoccus sacchari*) (Cockerell, 1895) (Hemiptera: Pseudococcidae) stands out, causing direct damage, such as shoot death, reduced growth, decreased weight, and reduced sucrose content, as well as indirect damage, including the transmission of pathogens and contamination by honeydew, which reduces the quality and productivity of the crop (Jayanthi et al., 2016; Monteiro, 2022). In general, pest monitoring relies mainly on manual inspection, and control is based on spraying insecticides, resulting in high costs and wasted resources (Monteiro, 2022). There is an urgent need to research precise monitoring and control. Remotely Piloted Aircraft (RPA) spectral remote sensing technology, combined with machine learning algorithms, can generate heat maps of insect pests, significantly improving the accuracy and timeliness of sucking pest monitoring (Ren et al., 2025). Comprehensive reviews of RPA flight experiments for vegetated areas emphasize that RPAs can deliver high-resolution, repeatable observations when platform/sensor choices and flight design are matched to the study's spatial-resolution needs; these reviews also summarize practical considerations for geometric and radiometric processing of RPA imagery (Salamí et al., 2014). Given that efficient sampling is necessary to mitigate the incidence of this pest and ensure the sustainability of production, advanced technologies, such as RPA, may provide high-precision sampling and mapping of *S. sacchari*.

With the evolution of RPA-based sampling technologies, new possibilities have emerged for environmental sampling, including enhanced spatial coverage and improved data collection efficiency (Khujamatov et al., 2025). RPAs enable crop condition monitoring, pesticide application, and the detection of problems during the vegetative cycle. However, despite these advancements, the application of RPA technology in insect monitoring faces significant challenges (Khujamatov et al., 2025). One of the primary benefits of imaging with this equipment is the generation of vegetation indices, such as the Normalized Difference Vegetation Index (NDVI) and the Normalized Difference Red Edge Index (NDRE) (Amarasingam et al., 2022). Reviews about vegetation indices show the spectral basis, typical applications, and limitations of standard indices — for example, NDVI's tendency to saturate at high canopy density and red-edge indices' greater sensitivity to changes in chlorophyll — and emphasize that index selection should be matched to canopy structure and the monitoring objective (Xue and Su, 2017). Understanding the relationship between vegetation indices derived from remote sensing and insect infestations could present an alternative and cost-effective tool for enhancing insect pest monitoring, targeted management, and improving decision-making (Mpisane et al., 2025). Studies have advocated further investigation into the relationship between early-season distributions of pests and important plant variables, such as NDVI, to better determine the strength of the correlations across years and sites. Other results indicate that NDRE also provides valuable information for crop monitoring in a timely and quantifiable manner (Choosumrong et al., 2023). Therefore, fundamental questions need to be formulated to determine whether the NDVI is more effective than the NDRE in addressing *S. sacchari* (Greene et al., 2021), as the relationship between insect-induced injury and vegetation index can vary among the feeding behaviors of pest species.

NDVI assesses vegetative vigor using the near-infrared and red spectral bands, detecting changes caused by factors such as water deficit and pest attacks (Peignier et al., 2023). The NDRE, calculated from the Red Edge and near-infrared bands, is indicated for larger crops, as it penetrates deeper into the plant canopy and offers greater sensitivity to photosynthetic activity (Bāders et al., 2022). Low values of both indices may indicate plant stress, including the presence of pests. Based on this, the present study aimed to detect patterns of *S. sacchari* occurrence in sugarcane crops using the NDVI and NDRE indices obtained via RPAs. The hypothesis tested is that low NDVI and NDRE indices reflect a high incidence of *S. sacchari*, allowing the indirect identification of the severity of the pest attack and supporting decision-making for its management. As the RPA-based sensing approach promises to be advantageous to sampling *S. sacchari* due to its low cost, high mobility, and flexible temporal and spatial resolution, we employed analysis to identify correlations between variables, including low and high infestations, and the NDVI and NDRE indices. This analysis created factors that represented a linear combination and prepared rankings by generating performance indexes based on these factors. To complement this analysis, we performed univariate machine learning analysis examining the Accuracy, Sensitivity, and Specificity of the relationship between NDVI or NDRE and low infestation levels versus high infestation levels. This is the first reported integration of NDVI and NDRE for detecting *S. sacchari*, with substantial implications for integrated management of this pest, and may be a basis for studies involving other pests in sugarcane.

2 Materials and methods

2.1 Study area

The study was conducted in the field at a sugarcane area of approximately 1.5 hectar on the Mandaú farm (7°02'0.47"S, 35° 6'2.82"W), located in the municipality of Alagoa Grande, State of Paraíba. The soil in the study area is classified as Eutrophic Red Nitossolo (Bdia–IBGE, 2023). According to Koppen, the

municipality's climate is classified as As, characterized by rainfall during the autumn and winter periods (Francisco and Santos, 2017). The average temperature and annual precipitation in this location are approximately 25.5 °C and 950 mm, respectively. The cultivated variety of the crop is RB 86 7515, which was in its first cultivation cycle as a sugarcane plant.

Crop management consisted of applying a pre-emergent herbicide (COMBINE 500 SC®) and a post-emergent herbicide (DONTOR®). Fertilization was based on phosphorus (P) and potassium (K), as well as the application of the bioproducts Canindé®, which contains *Trichoderma*, and Carcará®, which contains *Beauveria bassiana*, both manufactured by the company VSF Agricultura Sustentável e Comércio.

2.2 Sampling of *S. sacchari*

The monitoring of *S. sacchari* population density, including nymphs and adults, was conducted through surveys carried out in December 2023 and November 2024, to verify whether similar results were obtained over time. During this survey period, the sugarcane was in the final stage of stalk development, approximately 8 months after the planting date. The surveys consisted of random and zigzagging walks through the area to identify symptoms that characterize the pest, such as leaf yellowing caused by the scale insect. Given the resolution of the camera used and the size of the area, it was necessary to choose nine samples within the observational unit each year.

Each sampling point consisted of a perimeter of 10 m^2, where 20 plants were randomly chosen in a mirrored manner, that is, 10 plants in the left row and 10 plants in the right row, where the analyses and identification of the occurrence of the pest in question were performed, considering in each of the plants both the proportion of plants infested by the *S. sacchari* in the intensities: Low Level of Infestation (LIL) per plant, that is, less than 20 individuals (nymphs or adults) per plant, and High Level of Infestation (HIL), more than 20 individuals/plant, which characterized the occurrence of an insect colony. The level of infestation of *S. sacchari* was defined by the proportion of insects found in the 20 plants at each point. Coordinates of the location were obtained using a GPS device, allowing for the exact location of each point in its respective plot to be determined. From the ARP images, it was possible to observe the characteristics of the attacked plants in comparison to healthy plants.

2.3 Flights with ARP

The flights were performed with DJI's Mavic 3 multispectral Remotely Piloted Aircraft (RPA). The RPA has a set of 5 cameras, one RGB with a 4/3 CMOS sensor and 20MP, and other multispectral cameras that have four 1/2.8-inch single-band CMOS sensors, capable of taking 5 MP photos with a focal length equivalent to 25 mm and an aperture of f/2.0, and can obtain images in the bands: Green (G): 560 ± 16 nm, Red (R): 650 ± 16 nm, Red edge (RE): 730 ± 16 nm and Near-infrared (NIR): 860 ± 26 nm. This equipment also features a sensor located on its upper part that detects solar radiation in real time.

Combining this with the image information from each band of the multispectral camera provides more accurate reflectance values, which improves the consistency of the data collected across different regions, weather conditions, and times. In total, two flights were carried out, one each year, co-occurring with manual sampling, using a flight height set at 120 meters, taking the level of the takeoff point as a reference, and programmed for a sampling distance on the ground of approximately 4.3 cm/pixel, and frontal and lateral overlaps of 80% and 70% respectively.

2.4 Image processing

The multispectral image processing was performed using the Pix4d program. The multispectral images were loaded into the software. Then the processing began, which consists of three stages: initial processing, in which the program identifies analogous points between the images so that the images can be joined, as well as calibrating the internal parameters, such as the focal distance; in the second stage, the point cloud and mesh were generated; and finally, in the third and final stage, the digital elevation model (DSM), the orthomosaic and the indices were obtained.

Through image processing, the following indices were obtained: NDVI and NDRE. As mentioned previously, with these indices, it was possible to perform indirect observation and evaluation of the photosynthetic activity of the plants through an arithmetic calculation that uses the near-infrared (NIR) and red (Red) bands, in the case of NDVI, and the red edge (RedEdge) and red (Red) bands for NDRE. By obtaining these two indices, it was also possible to compare the degree of relationship of each one in identifying the *S. sacchari* in the crop.

2.5 Obtaining NDVI and NDRE values from plants analyzed in the field

The NDVI and NDRE values of the infested plants were obtained using QGIS software, version 3.34.0. After processing the images and obtaining the orthomosaics in tif format, they were added to QGIS, and later, the GPS points obtained in fields at the pest sampling sites were also added. Using these points, a buffer was created for each of them to delimit a specific area, which in the present study was 2 m^2. Finally, the zonal statistics function was used, which calculates statistics on the values of a raster (image or degree of values) within regions defined by a vector (buffer). This resulted in the average value of approximately 3600 pixels per area being obtained.

2.6 Statistical analysis

All analyses were conducted using R software (R Core Team, 2024). The scatter plots were created using the ggscatter function

(Kassambara, 2023), which allows varying several parameters depending on the desired result. To add the correlation coefficient with P values to the scatter plot, the stat_cor function was used, where the Pearson method was defined for analyzing the data in this study. In this type of correlation, the result obtained is the Pearson correlation coefficient (r), which is nothing more than a dimensionless measure that can assume values in the range between -1 and +1 and measures the intensity and direction of linear relationships, where the intensity refers to the degree of relationship between two variables, that is, the closer the r values are to the extremes of the range (-1 and +1), the stronger the correlation between these variables, while the closer to the center of the range (0), the weaker the linear correlation.

A component factor analysis model was programmed in the R language for this study using the package stats from the basis of R software (R Core Team, 2024), due to the occurrence of relatively high correlation coefficients. For this analysis, a multivariate index was calculated that could capture the joint behavior of the original values of the low and high pest infestation variables. The LIL and HIL infestation values were used as references, along with the values of the NDRE and NDVI indices and the variance shared by each factor in the principal components analysis. The results were expressed in a biplot.

To build the ranking from factor analysis, we used the weighted rank-sum criterion, in which, for each observation, the values of all factors obtained (that have eigenvalues greater than 1) are weighted by the respective proportions of shared variance and added, with the subsequent ranking of the observations based on the results obtained. This criterion is widely accepted because it considers the performance of all the original variables, as only considering the first factor (principal factor criterion) may overlook positive performance, for instance, in a specific variable that shares a considerable proportion of variance with the second factor. Additionally, statistics from the confusion matrix related to modelling vegetation indices as a function of the low and high infestation levels were used, and the following metric statistics were captured: Accuracy, Sensitivity, and Specificity of the models. We used the confusionMatrix function to calculate a cross-tabulation of observed and predicted classes, along with associated statistics (Kuhn, 2008).

3 Results

Table 1 presents the mean values of the proportion of plants infested by *S. saccharis* at the LIL (low), HIL (high), NDVI, and NDRE levels, along with their respective measures of variability, specifically Standard Deviation (SD) and/or 95% Confidence Intervals ($CI_{95\%}$) within the two years of research. In the first year, the LIL had mean values of absolute infestation that varied from 0.85 ($CI_{95\%}$: 0.76-0.93) to 0.55 ($CI_{95\%}$: 0.43-0.66), with less variability in the highest means of absolute infestation (SD = 0.36). In contrast, for the lowest level of absolute infestation, greater data variability was observed (SD = 0.51). For the same period, the HIL values ranged from 0.10 ($CI_{95\%}$ = 0.03-0.16) to 0.65 ($CI_{95\%}$ = 0.54-0.75).

In the first year of research, the NDVI data had averages ranging from 0.56 to 0.70. Similar behavior was observed in NDRE. In the second year of study, the mean absolute infestation values for LIL ranged from 0.70 ($CI_{95\%}$ = 0.47-0.92) to 0.35 ($CI_{95\%}$ = 0.12 - 0.58). For HIL in the same period, values ranged between 0.15 ($CI_{95\%}$ = -0.02 - 0.32) and 0.60 ($CI_{95\%}$ = 0.36 - 0.83). In the case of NDVI in the second year, the averages ranged from 0.64 to 0.72, with low variability at all points analyzed (standard deviation ranging from 0.04 to 0.08). NDRE exhibited similar behavior, with average values ranging from 0.36 to 0.45 and standard deviations (SD) ranging from 0.03 to 0.05. We observed in Table 1 that the highest scores were associated with low values of LIL and HIL, as well as high values of NDVI and NDRE. A similar result can be observed in the lowest values of the scores, characterized by high levels of LIL and HIL, and low values of NDVI and NDRE (Table 1). According to the estimated dispersion parameter, a value lower than one indicates evidence of non-overdispersion in the observed data for all variables (Table 1).

Figure 1 shows the NDRE orthomosaic, along with its corresponding value scale. The values ranged from 0.21 to 0.49, with lower values corresponding to areas with the lowest photosynthetic activity and higher values corresponding to regions with the highest photosynthetic activity. The areas that presented the lowest index values were those with *S. sacchari* infestation, indicating influence of the insect pest on the plant's vegetative activity.

Figure 2 shows the NDVI orthomosaic and its scale of values obtained in the study area. The values ranged from 0.44 to 0.88, representing the areas of lowest and highest vegetative activity of the crop. The NDVI orthomosaic exhibits greater saturation in the index values compared to the NDRE. In agreement with the NDRE data, the locations that presented the lowest NDVI values were those with the highest incidence of the insect *S. sacchari*.

By relating the infestation data to the vegetation index data, it was possible to observe that the highest proportions of LIL were associated with the lowest levels of NDRE, with a similar result observed between HIL and NDVI (Table 1). As shown in Figure 3a, a strong and negative correlation was observed between NDRE and LIL (r = -0.72), indicating that they are inversely proportional. The P-value was significant (<5%), with a value of 0.00047, indicating a statistically significant correlation. In Figure 3b, a correlation is observed between NDRE and HIL. This analysis presented a correlation of -0.43 and a P value of 0.06 (>5%), indicating that the two variables are also inversely proportional; however, this correlation lacked significance, suggesting that NDRE does not present an effective relationship in the indirect detection of colonies. Figure 3c shows the graphical representation of the correlation between the NDVI and the level of *S. sacchari* infestation. The figure shows that the correlation was negative (-0.62), indicating that the two variables are inversely proportional. However, the correlation was not considerably high when compared with the NDVI and HIL variables. The *r-value* in this analysis was -0.72, thereby revealing a significant correlation between NDVI and HIL (Figure 3d).

Figure 4 presents a multivariate correlation network that expresses a scale of colors, indicating the behavior and

TABLE 1 Proportion of infested plants at low (LIL) and high (HIL) levels, vegetative indices NDVI and NDRE, and ranking based on score-values of the factorial analysis from Pearson's correlation matrix.

Mean ± SD ($CI_{95\%}$)		Mean ± SD		F1	F2	Score
LIL	HIL	NDVI	NDRE			
0.35 ± 0.48 (0.12-0.58)	0.15 ± 0.37 (-0.02-0.32)	0.72 ± 0.04	0.45 ± 0.03	1.73	-0.35	1.16
0.40 ± 0.50 (0.16-0.63)	0.25 ± 0.44 (0.04-0.45)	0.72 ± 0.05	0.43 ± 0.03	1.30	-0.58	0.82
0.45 ± 0.51 (0.21-0.69)	0.20 ± 0.41 (0.008-0.39)	0.70 ± 0.06	0.44 ± 0.03	1.22	-0.29	0.81
0.35 ± 0.48 (0.12-0.58)	0.20 ± 0.41 (0.008-0.39)	0.70 ± 0.06	0.37 ± 0.04	0.82	0.07	0.59
0.50 ± 0.51 (0.26-0.74)	0.25 ± 0.44 (0.04-0.46)	0.71 ± 0.05	0.38 ± 0.03	0.64	0.26	0.49
0.65 ± 0.48 (0.54-0.75)	0.10 ± 0.30 (0.03-0.16)	0.67 ± 0.05	0.37 ± 0.02	0.22	1.66	0.43
0.55 ± 0.51 (0.43-0.66)	0.30 ± 0.47 (0.19-0.40)	0.69 ± 0.06	0.39 ± 0.02	0.37	-0.08	0.25
0.75 ± 0.44 (0.65-0.84)	0.25 ± 0.44 (0.15-0.34)	0.70 ± 0.05	0.37 ± 0.02	0.04	1.25	0.24
0.55 ± 0.51 (0.43-0.66)	0.35 ± 0.48 (0.24-0.45)	0.70 ± 0.05	0.39 ± 0.03	0.37	-0.34	0.20
0.45 ± 0.51 (0.21-0.69)	0.40 ± 0.50 (0.16-0.63)	0.69 ± 0.04	0.39 ± 0.04	0.37	-1.09	0.08
0.50 ± 0.51 (0.26-0.74)	0.35 ± 0.49 (0.12-0.57)	0.69 ± 0.04	0.36 ± 0.03	0.12	-0.26	0.04
0.85 ± 0.36 (0.76-0.93)	0.25 ± 0.44 (0.15-0.34)	0.66 ± 0.06	0.37 ± 0.03	-0.47	1.40	-0.10
0.75 ± 0.44 (0.65-0.84)	0.25 ± 0.44 (0.15-0.34)	0.65 ± 0.05	0.34 ± 0.03	-0.63	1.29	-0.23
0.65 ± 0.49 (0.42-0.88)	0.40 ± 0.50 (0.16-0.64)	0.65 ± 0.06	0.38 ± 0.04	-0.40	-0.45	-0.36
0.85 ± 0.36 (0.76-0.93)	0.40 ± 0.50 (0.28-0.51)	0.67 ± 0.06	0.35 ± 0.03	-0.81	0.71	-0.45
0.85 ± 0.36 (0.76-0.93)	0.40 ± 0.50 (0.28-0.51)	0.67 ± 0.06	0.32 ± 0.03	-1.05	1.03	-0.57
0.60 ± 0.50 (0.36-0.84)	0.55 ± 0.51 (0.31-0.79)	0.64 ± 0.06	0.39 ± 0.03	-0.58	-1.76	-0.70
0.70 ± 0.47 (0.47-0.92)	0.60 ± 0.50 (0.36-0.83)	0.67 ± 0.08	0.38 ± 0.05	-0.66	-1.43	-0.70
0.80 ± 0.41 (0.70-0.89)	0.65 ± 0.48 (0.54-0.75)	0.56 ± 0.06	0.29 ± 0.03	-2.61	-1.02	-2.02
$\delta^2_{\text{binomial model}}$= 0.0361	$\delta^2_{\text{binomial model}}$= 0.0699	$\delta^2_{\text{gauss model}}$=0.0130	$\delta^2_{\text{gauss model}}$=0.0114			

Mean: arithmetic means. SD, standard deviation; 95% CI, confidence intervals with a 95% probability; LIL, Low Infestation Level, characterized by fewer than 20 insects; HIL, High Infestation Level, characterized by an infestation with more than 20 insects; NDVI, Normalized Difference Vegetation Index; NDRE, Normalized Difference Red Border Index; F1, Factor 1; F2, Factor 2; Score, Score from the machine learning principal component factor analysis.

relationship between the analyzed variables. A directly proportional manifestation was observed between the NDVI and NDRE indices, as well as between LIL and HIL, although the latter is weak, with values close to zero. Additionally, NDVI and NDRE exhibit inverse correlations with HIL and LIL, respectively.

In another multivariate perspective, the data were also analyzed using unsupervised Machine Learning methods, specifically PCA and factorial analysis. In the first case, it was observed that two components explained 89.56% of the data variation, with the first component accounting for 71.17% (λ = 0.7117) of this variation, exhibiting higher eigenvector loadings for the vegetative indices NDVI (v = 0.5293) and NDRE (v = 0.5689). On the other hand, the variables LIL and HIL presented greater relationships with the second principal component, with eigenvector loadings (v) of -0.8308 and 0.4902, respectively (Figure 5).

According to the trigonometric analysis of the arrangement of vectors in the factor analysis biplot, mediated by the cosine of the angle θ, negative relationships are reinforced (cosine of the angle $\theta > 130° = r > 0.60$) between the variables LIL versus NDRE and NDVI versus HIL, as well as a low relationship between NDVI and LIL and between NDRE versus HIL (cosine of the angle $\theta < 130° = r < 0.60$) (Figure 6). 71.17% of the total variance is shared to form the first factor [LIL: -0.4907; HIL: -0.4409; NDVI: 0.5383; and NDRE: 0.5243], and 18.39% of the total variance is shared to form the second factor [LIL: -0.5195; HIL: 0.7693; NDVI: -0.1668; and NDRE: 0.3321]. While the variables NDVI and NDRE showed stronger correlations with the first factor, we can see that only the variables LIL and HIL showed stronger correlations with the second factor.

In the modelling of vegetation indices as a function of the low and high infestation levels, Kappa coefficients (> 0.80) approaching infestation levels, as indicated by NRDE and NDVI, yielded excellent results. In addition, the statistical test comparing the model's accuracy to the No Information Rate (NIRT) reported a small p-value less than 0.05, indicating that the model's accuracy is significantly better than the NIRT. The Accuracy was high when NDVI was modeled as a function of LIL or HIL, but it was low when NDRE was tested as a function of HIL, and high when LIL was used. It means that the proportion of correctly classified instances (both true positives and true negatives) out of the total number of cases is

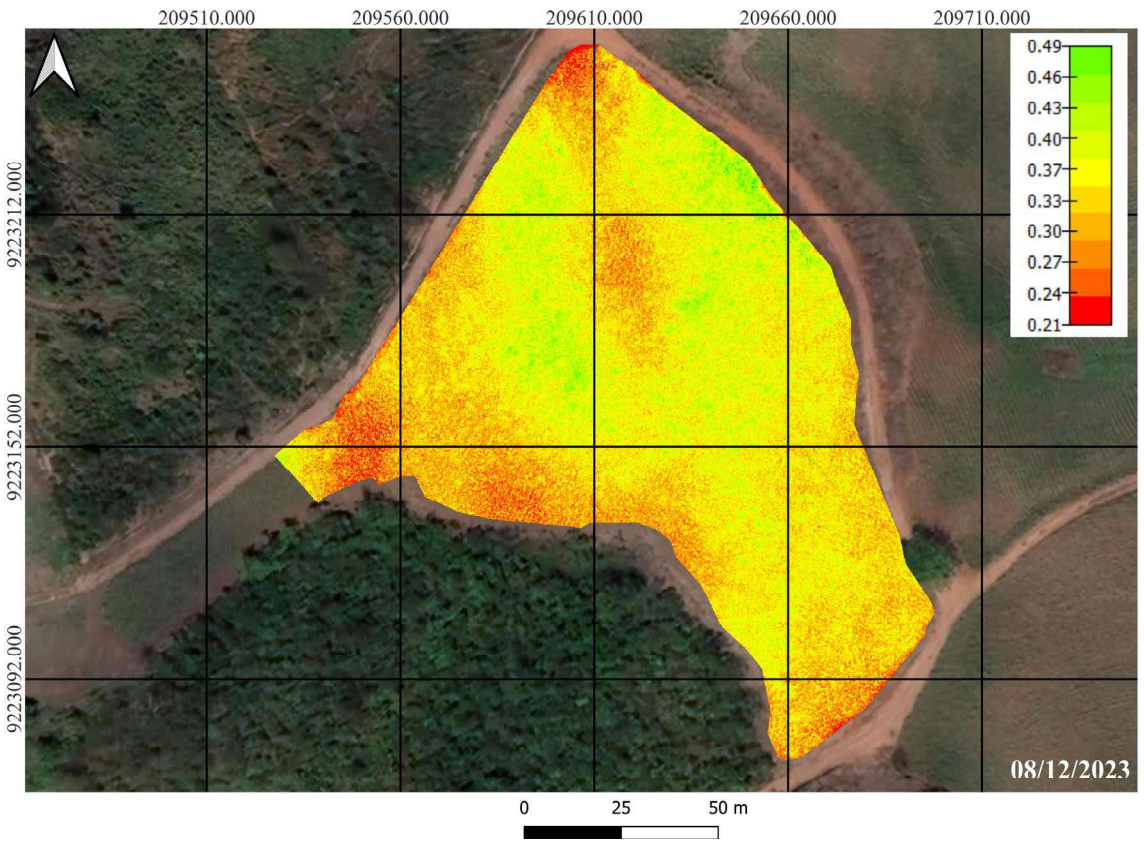

FIGURE 1
Normalized Difference Red Edge Vegetation Index ortho mosaic from the study area. Images captured by ARP M3M at the Mandaú farm, located in Alagoa Grande, PB, during the 3rd stage of sugarcane development. The red spots also indicate *Saccharicoccus sacchari* infestation.

low when there is a low or high density of *S. sacchari*. Still, for NDRE, it is proper only when there is a low density of *S. sacchari*. The recall, or sensitivity, which is the true positive rate from the confusion matrix, measures the model's ability to identify a positive relationship between infestation and the indices correctly, specifically with respect to NDVI and NDRE. This index indicates the proportion of actual positive cases that are correctly classified as positive by the model, primarily in the cases of HIL and LIL, respectively. The Specificity measure values revealed the models' ability to correctly identify negative cases by minimizing false positives in the relationships between NDVI and LIL, between NDVI and HIL, and between NDRE and LIL (Table 2).

4 Discussion

Although the study was conducted in an area of 1.5 ha, the results of this research indicated that, depending on the intensity of *S. sacchari* infestation, there is evidence of differences in the reflectance of the spectral bands used to calculate the vegetation indices. Based on the factor analysis loads and the percentage of explanation of each component (F1 and F2), it was possible to propose the construction of a multivariate index capable of jointly estimating the levels of infestation (high and low) and the vegetative indices NDVI and NDRE. The univariate and multivariate analyses revealed negative relationships between the variables LIL versus NDRE, as well as between NDVI versus HIL. Additionally, there was a low relationship between NDVI and LIL, and between NDRE and HIL. The highest scores were associated with low values of LIL and HIL, as well as high values of NDVI and NDRE. This result suggests that a multivariate combination involving these parameters may be used in further management decision-making based on the degree of infestation integrated with vegetation indices. In addition, a high cumulative variance (more than 80%) explained by only two factors from the unsupervised factorial machine learning model indicated a highly accurate representation of the data's variability. However, it is worth emphasizing that the variability in larger or different agroecological zones may affect the outcomes.

The measures of the relationships between NDVI and HIL, NDVI and LIL, as well as between NDRE and LIL, captured by the supervised machine learning models, revealed low false negatives and/or false positives from the confusion matrix in the relationship between vegetation indices and insect infestation. Confusion matrix results show weaker performance for NDRE in high infestations (Accuracy = 44.9%); hence, NDRE can fail to detect hotspots of insect injury when *S. sacchari* is in conditions with high infestation per plant. Thus, the use of this index in situations of high *S. sacchari* density can have severe consequences. Therefore, in the present

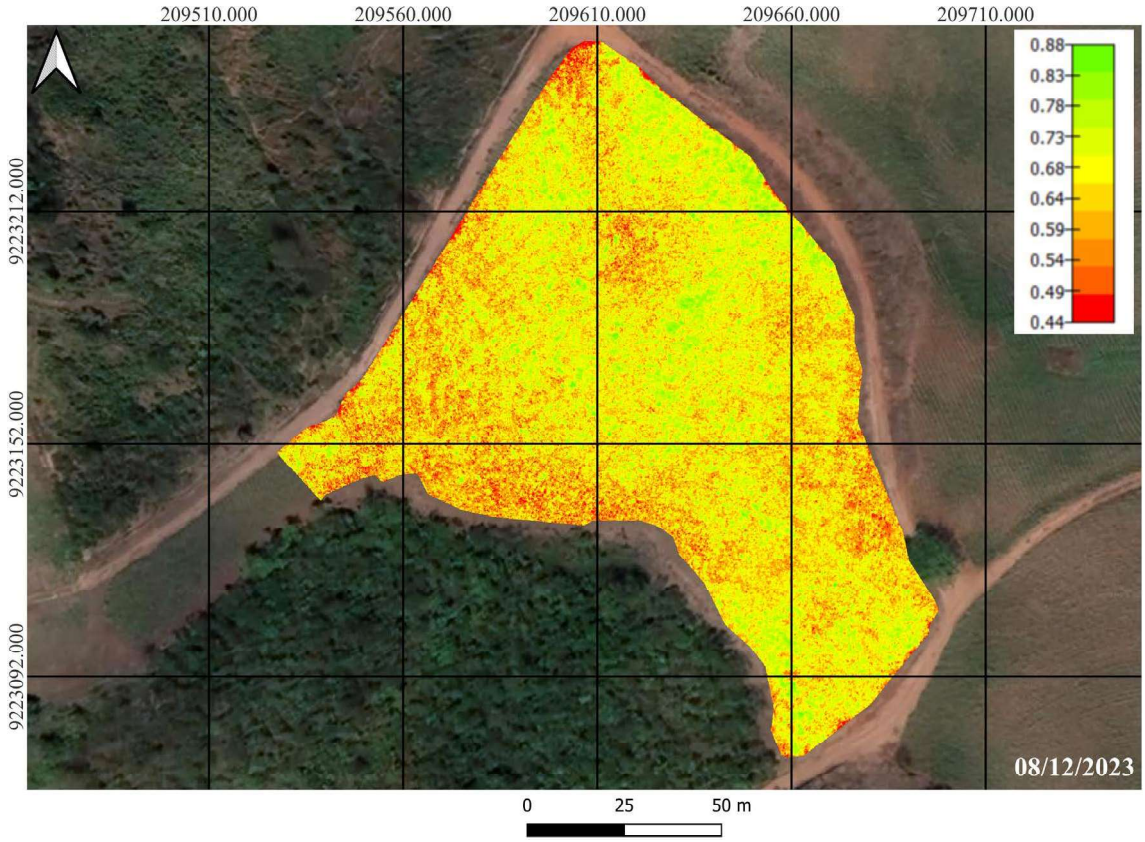

FIGURE 2
Orthomosaic of the Normalized Difference Vegetation Index of the study area. Images captured by ARP M3M on the Mandaú farm, located in Alagoa Grande, PB, during the 3rd stage of sugarcane development. The red spots also indicate *Saccharicoccus sacchari* infestation.

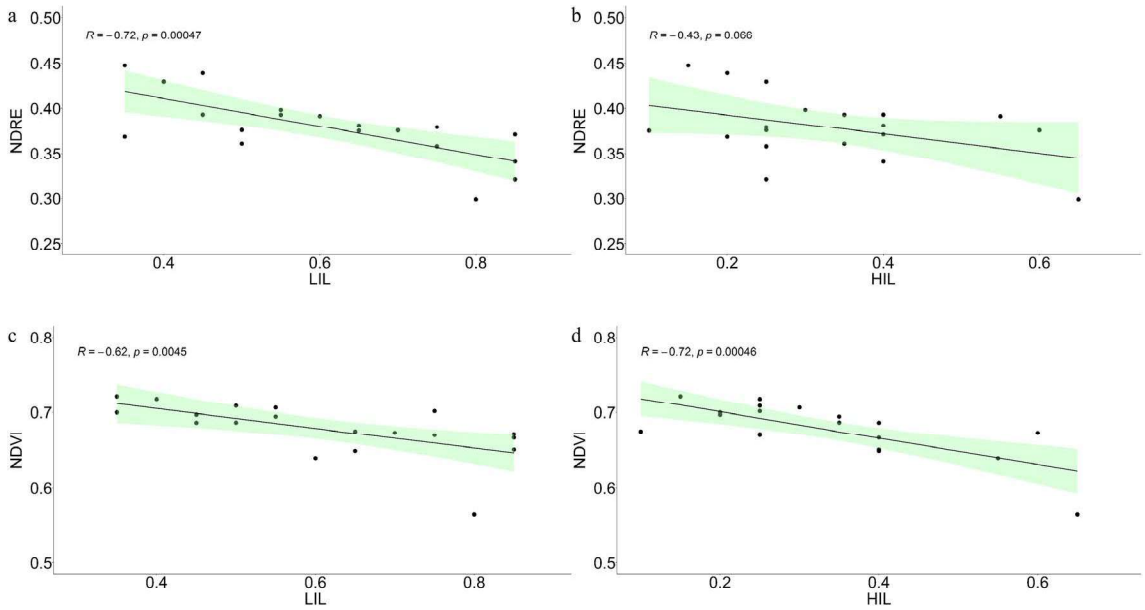

FIGURE 3
Correlation between Normalized Difference Red Edge Vegetation Index (NDRE) and Low Infestation Level (LIL) of *Saccharicoccus sacchari* **(a)**; Correlation between Normalized Difference Red Edge Vegetation Index (NDRE) and High Infestation Level (HIL) of *S. sacchari* **(b)**; Correlation between NDVI and LIL of *S. sacchari* **(c)**; Correlation between NDVI and HIL of *S. sacchari* **(d)**.

FIGURE 4
Correlation network between the Normalized Difference Vegetation Index (NDVI), the Normalized Difference Red Edge Vegetation Index (NDRE), both obtained through multispectral images, and low (LIL) and high (HIL) infestation indices of *Saccharicoccus sacchari* in sugarcane plants located at the Mandaú farm, Alagoa Grande - PB.

study, it was found that the NDRE was efficient in detecting areas with only low levels of insect infestation (fewer than 20 insects/plant). On the other hand, the index was not efficient in identifying regions with insect colonies (more than 20 insects/plant). According to Boiarskii and Hasegawa (2019), NDVI may be an indicator of a visible green color wherever vegetation is present; NDRE could be an indicator of nitrogen limitation in the leaves. NDRE identified areas of low chlorophyll content even when NDVI was uniform, clear evidence of increased sensitivity to invisible stresses. These observed behaviors are consistent with general properties of vegetation indices discussed in review literature: red-edge indices often show higher sensitivity to changes in chlorophyll content at early stress stages, whereas NDVI can saturate at high leaf area index, which explains why different indices can be complementary for early vs. advanced damage detection (Xue and Su, 2017). As pointed out by Dash et al. (2017), this limitation may be associated with the characteristics of the NDRE, which is extremely sensitive to initial changes in chlorophyll concentration. When the infestation is mild, the index can detect subtle changes, such as the initial decrease in chlorophyll and changes in leaf color. However, in situations of high infestation, where damage is more severe (resulting in a drastic reduction in chlorophyll and reduced growth), the NDRE response loses accuracy, possibly due to saturation or limitations in identifying more severe changes. Based on the detection of the monitoring window for pine wilt disease using multi-temporal with multispectral imagery and

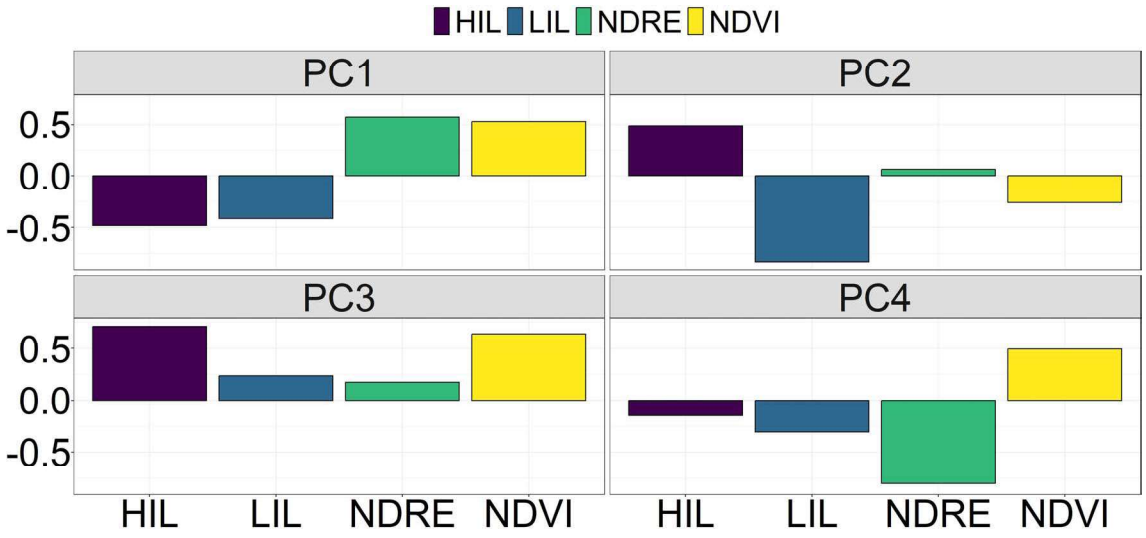

FIGURE 5
Eigenvector loadings of the variables High Level of Infestation (HIL), Low Level of Infestation (LIL) of *Saccharicoccus sacchari*, Normalized Difference Red Edge Index (NDRE), and Normalized Difference Vegetation Index (NDVI) associated with the principal components.

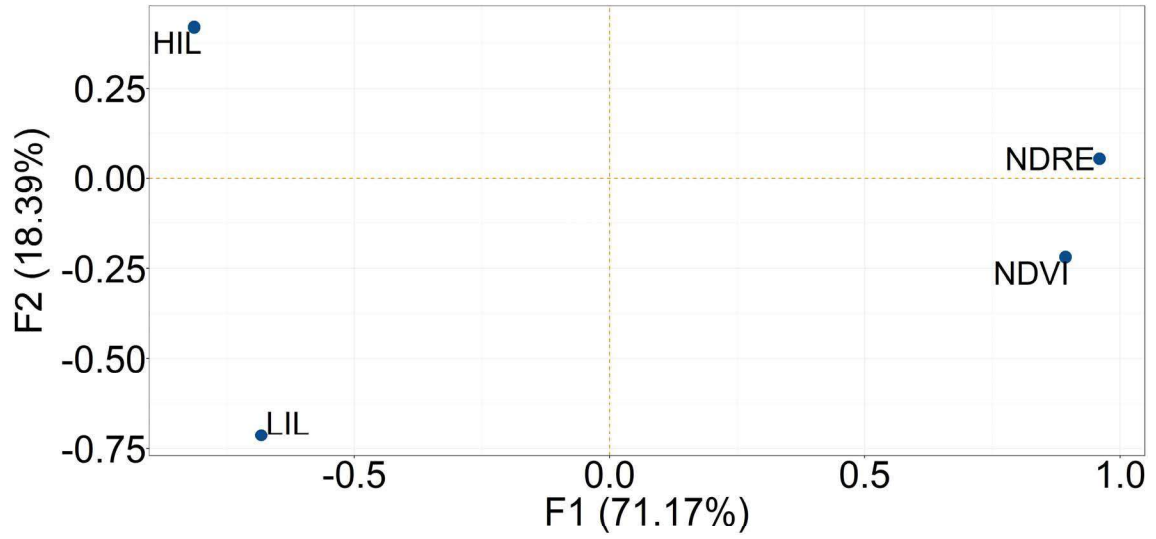

FIGURE 6
Factorial analysis of the variables High Level of Infestation (HIL), Low Level of Infestation (LIL), Normalized Difference Red Edge Index (NDRE), and Normalized Difference Vegetation Index (NDVI).

machine learning algorithms, Wu et al. (2023) found that NDRE was identified as the best index for early detection of the disease, precisely in the initial phase called "green attack stage", while NDVI appears later in the intermediate/final phases. In some cases, NDRE can identify areas of low chlorophyll content even when NDVI was uniform, highlighting clear evidence of increased sensitivity to invisible stresses (Marx and Kleinschmit, 2017).

On the other hand, the NDVI index demonstrated effectiveness in detecting areas with high population densities of *S. sacchari* but was limited in identifying light infestation. NDVI failed to accurately indicate the proportion of true positive cases that the model correctly classifies as positive in the confusion matrix, particularly when relating NDVI and LIL. This behavior can be explained by the characteristic of NDVI to saturate in situations of high chlorophyll concentration, as described by Arapostathi et al. (2024). In places where the infestation was low, the changes in chlorophyll were subtle, making detection by NDVI difficult. However, in areas of high infestation, the damage caused by the insect pest resulted in a significant reduction in chlorophyll and lower vegetative growth. Hence, the index was efficient in identifying these conditions.

TABLE 2 Statistics from the confusion matrix related to modelling vegetation indices as a function of the low and high infestation levels.

Metric statistics	NDVI		NDRE	
	LIL	HIL	LIL	HIL
Accuracy	80.00%	80.33%	73.33%	44.90%
Sensitivity	62.50%	81.57%	83.33%	25.00%
Specificity	99.99%	99.99%	66.67%	90.90%
Kappa coefficient	81.00%	83.00%	90.00%	34.00%
P-Value [Acc > NIRT]	0.03209	0.0450	0.0217	0.6304

NDVI, Normalized Difference Vegetation Index; NDRE, Normalized Difference Red Edge Index; HIL, High Level of Infestation; LIL, Low Level of Infestation.

The results of this study corroborate the findings of Bárta et al. (2022), who demonstrated that NDRE is more effective than NDVI in detecting infestations earlier, due to the sensitivity of the red-edge spectral band to early changes. Similarly, in this research, NDRE was effective in detecting subtle damage caused by *S. sacchari*, while NDVI was better suited to identify areas with severe damage. Although NDRE and NDVI indices have shown usefulness in detecting *S. sacchari* infestations, a significant limitation is that the injuries caused by the pest can be confused with symptoms caused by other pests, pathogens, or water stress. Therefore, field monitoring is essential to confirm the cause of the damage and validate the spectral patterns associated with *S. sacchari*.

The results reinforce the potential of vegetation indices to support integrated pest management strategies in sugarcane crops. The ability of NDRE to detect early infestations can aid in preventive monitoring, while NDVI can be used in more advanced stages, when damage is more severe. The use of these tools enables more assertive and timely decision-making, contributing to more efficient crop management. Future studies could extend the monitoring period and include a larger number of samples to further validate the results, including using an external dataset or cross-validation, In addition, it is recommended to investigate the relationship between vegetation indices and other physiological variables, such as leaf water content and photosynthesis rate, to obtain a more comprehensive understanding of the impacts of *S. sacchari* infestation and improve the accuracy of remote sensing diagnoses.

Thus, it is concluded from this research that suborbital remote sensing combined with the vegetation indices NDVI and NDRE is effective for identifying patterns related to injuries caused by *S. sacchari* in sugarcane crops, proving to be an effective tool for

monitoring this insect pest. The use of both indices together is recommended for detecting the occurrence of *S. sacchari*, as they complement each other in identifying the intensity of pest infestation.

Data availability statement

The raw data supporting the conclusions of this article will be made available by the authors, without undue reservation.

Author contributions

AS: Formal analysis, Software, Writing – original draft, Methodology, Data curation, Visualization, Conceptualization, Validation, Project administration, Investigation, Supervision, Funding acquisition, Writing – review & editing, Resources. RO: Writing – review & editing, Writing – original draft, Conceptualization. JN: Writing – review & editing, Funding acquisition, Writing – original draft, Formal analysis, Investigation, Data curation, Resources, Conceptualization, Project administration, Methodology. VB: Resources, Writing – review & editing, Funding acquisition, Supervision, Software, Methodology, Project administration, Formal analysis, Writing – original draft, Data curation, Visualization, Conceptualization, Validation, Investigation. MG: Methodology, Supervision, Software, Conceptualization, Writing – review & editing, Investigation, Validation, Formal analysis, Writing – original draft, Funding acquisition. AA: Conceptualization, Writing – review & editing, Writing – original draft, Data curation. RS: Writing – original draft, Writing – review & editing. AN: Project administration, Writing – review & editing, Visualization, Writing – original draft, Methodology, Formal analysis, Data curation, Validation, Supervision, Conceptualization, Investigation, Funding acquisition, Software, Resources. JM: Writing – review & editing, Methodology, Writing – original draft, Supervision, Software, Funding acquisition, Investigation, Visualization, Resources, Validation, Formal analysis, Project administration, Data curation, Conceptualization.

Funding

The author(s) declare financial support was received for the research and/or publication of this article. The authors acknowledge the Conselho Nacional de Desenvolvimento Científico e Tecnológico (CNPq) for supporting the project (Process number: 420064/2023–0 and 308296/2025-7), and the Coordenação de Aperfeiçoamento de Pessoal de Nível Superior-Brasil (CAPES) for providing grants and research funding.

Conflict of interest

The authors declare that the research was conducted in the absence of any commercial or financial relationships that could be construed as a potential conflict of interest.

Generative AI statement

The author(s) declare that no Generative AI was used in the creation of this manuscript.

Any alternative text (alt text) provided alongside figures in this article has been generated by Frontiers with the support of artificial intelligence and reasonable efforts have been made to ensure accuracy, including review by the authors wherever possible. If you identify any issues, please contact us.

Publisher's note

References

Amarasingam, N., Salgadoe, A. S. A., Gonzalez, L. F., Powell, K., and Natarajan, S. (2022). 'A review of UAV platforms, sensors, and applications for monitoring of sugarcane crops'. *Remote Sens. Applications: Soc. Environ.* 26, 100712. doi: 10.1016/j.rsase.2022.100712

Arapostathi, E., Panopoulou, C., Antonopoulos, A., Katsileros, A., Karellas, K., Dimopoulos, C., et al. (2024). 'Early detection of potential infestation by *Capnodis tenebrionis* (L.) (Coleoptera: Buprestidae), in stone and pome fruit orchards, using multispectral data from a UAV'. *Agronomy* 14, 20. doi: 10.3390/agronomy14010020

Bāders, E., Romāns, E., Desaine, I., Krišāns, O., Seipulis, A., Donis, J., et al. (2022). 'An integration of linear model and "random forest" techniques for prediction of Norway spruce vitality: a case study of the hemiboreal forest, Latvia'. *Remote Sens.* 14, 2122. doi: 10.3390/rs14092122

Bárta, V., Hanuš, J., Dobrovolný, L., and Homolová, L. (2022). 'Comparison of field survey and remote sensing techniques for detection of bark beetle-infested trees'. *For. Ecol. Manage.* 506, 119984. doi: 10.1016/j.foreco.2021.119984

Bdia–IBGE (2023). Banco de Dados de Informações Ambientais. Available online at: https://bdia.ibge.gov.br (Accessed September 20, 2025).

Boiarskii, B., and Hasegawa, H. (2019). 'Comparison of NDVI and NDRE indices to detect differences in vegetation and chlorophyll content'. *J. Mechanics Continua Math. Sci.* 4, 20–29. doi: 10.26782/jmcms.spl.4/2019.11.00003

Choosumrong, S., Hataitara, R., Sujipuli, K., Weerawatanakorn, M., Preechaharn, A., Premjet, D., et al. (2023). 'Bananas diseases and insect infestations monitoring using multi-spectral camera RTK UAV images'. *Spatial Inf. Res.* 31, 371–380. doi: 10.1007/s41324-022-00504-y

Conab – Companhia Nacional de Abastecimento (2024). Acompanhamento da safra brasileira de cana-de-açúcar. Available online at: https://www.conab.gov.br (Accessed September 20, 2025).

Dash, J. P., Watt, M. S., Pearse, G. D., Heaphy, M., and Dungey, H. S. (2017). 'Assessing very high resolution UAV imagery for monitoring forest health during a simulated disease outbreak'. *ISPRS J. Photogrammetry Remote Sens.* 131, 1–14. doi: 10.1016/j.isprsjprs.2017.07.007

Francisco, P. R. M., and Santos, D. (2017). Climatologia do Estado da Paraíba (Campina Grande: EDUFCG). Available online at: https://livros.editora.ufcg.edu.br/index.php/edufcg/catalog/book/131.

Greene, A. D., Reay-Jones, F. P., Kirk, K. R., Peoples, B. K., and Greene, J. K. (2021). 'Spatial associations of key lepidopteran pests with defoliation, NDVI, and plant height in soybean'. *Environ. Entomology* 50, 1378–1392. doi: 10.1093/ee/nvab098

Jayanthi, R., Srikanth, J., and Sushil, S. N. (2016). "'Sugarcane'," in *Mealybugs and Their Management in Agricultural and Horticultural Crops*. Eds. M. Mani and C. Shivaraju (India: Springer India), 287–296. doi: 10.1007/978-81-322-2677-2_28

Kassambara, A. (2023). ggpubr: 'ggplot2' Based Publication Ready Plots. R package version 0.6.0. Available online at: https://CRAN.R-project.org/package=ggpubr (Accessed December 24, 2024).

Khujamatov, H., Muksimova, S., Abdullaev, M., Cho, J., and Jeon, H.-S. (2025). 'Advanced insect detection network for UAV-based biodiversity monitoring'. *Remote Sens.* 17, 962. doi: 10.3390/rs17060962

Kuhn, M. (2008). 'Building predictive models in R using the caret package'. *J. Stat. Software* 28. doi: 10.18637/jss.v028.i05

Marx, A., and Kleinschmit, B. (2017). 'Sensitivity analysis of RapidEye spectral bands and derived vegetation indices for insect defoliation detection in pure Scots pine stands'. *iForest - Biogeosciences Forestry* 10, 659–668. doi: 10.3832/ifor1727-010

Monteiro, G. G. (2022). Desenvolvimento biológico, danos diretos e indiretos da cochonilha rosada de cana-de-açúcar Saccharicoccus sacchari (Cockerell 1895) (Hemiptera: Pseudococcidae) no estado de São Paulo: biossistemática da cochonilha rosada de cana-de-açúcar (Universidade Estadual Paulista (UNESP). Available online at: https://repositorio.unesp.br/items/b29210ae-e599-42db-b7ec-91f9f137690d.

Mpisane, K., Kganyago, M., Munghemezulu, C., Price, R., and Nduku, L. (2025). 'A systematic review of remote sensing technologies and techniques for agricultural insect pest monitoring: lessons for *Locustana pardalina* (Brown Locust) control in South Africa'. *Front. Remote Sens.* 6. doi: 10.3389/frsen.2025.1571149

Peignier, S., Lacotte, V., Duport, M. G., Baa-Puyoulet, P., Simon, J. C., Calevro, F., et al. (2023). 'Detection of aphids on hyperspectral images using one-class SVM and Laplacian of Gaussians'. *Remote Sens.* 15, 2103. doi: 10.3390/rs15082103

R Core Team (2024). *R: A language and environment for statistical computing* (Vienna: R Foundation for Statistical Computing). Available online at: https://www.R-project.org/ (Accessed December 2, 2024).

Ren, C., Liu, B., Liang, Z., Lin, Z., Wang, W., Wei, X., et al. (2025). 'An innovative method of monitoring cotton aphid infestation based on data fusion and multi-source remote sensing using unmanned aerial vehicles'. *Drones* 9, 229. doi: 10.3390/drones9040229

Salamí, E., Barrado, C., and Pastor, E. (2014). 'UAV flight experiments applied to the remote sensing of vegetated areas'. *Remote Sens.* 6, 11051–11081. doi: 10.3390/rs61111051

Shang, X.-K., Wei, J.-L., Pan, X.-H., Huang, C.-H., and Nikpay, A. (2024). 'Sugarcane insect pests in China: species, distribution and population dynamics'. *Sugar Tech* 26, 20–32. doi: 10.1007/s12355-023-01325-5

Silva, B. F., and Cavichioli, F. A. (2022). 'O uso de veículos aéreos não tripulados para detecção de pragas e doenças na cultura da soja'. *Rev. Interface Tecnológica* 19, 236–247. doi: 10.31510/infa.v19i1.1363

Wu, D., Yu, L., Yu, R., Zhou, Q., Li, J., Zhang, X., et al. (2023). 'Detection of the monitoring window for pine wilt disease using multi-temporal UAV-based multispectral imagery and machine learning algorithms'. *Remote Sens.* 15, 444. doi: 10.3390/rs15020444

Xue, J., and Su, B. (2017). 'Significant remote sensing vegetation indices: a review of developments and applications'. *J. Sensors* 2017, 1353691. doi: 10.1155/2017/1353691